NeuroImage 43 (2008) 192–203

Contents lists available at ScienceDirect

NeuroImage

journal homepage: www.elsevier.com/locate/ynimg

The multiple synaesthete E.S. — Neuroanatomical basis of interval-taste and tone-colour synaesthesia

Jürgen Hänggi *, Gian Beeli, Mathias S. Oechslin, Lutz Jäncke *

Division of Neuropsychology, Institute of Psychology, University of Zurich, Binzmühlestrasse 14, 8050 Zurich, Switzerland

ARTICLE INFO

Article history:
Received 17 November 2007
Revised 1 June 2008
Accepted 6 July 2008
Available online 22 July 2008

ABSTRACT

Synaesthesia is the involuntary physical experience of a crossmodal linkage such as when hearing a tone evokes the additional sensation of seeing a colour. We previously described a professional musician with absolute pitch perception who experiences both different tastes in response to hearing different tone intervals (e.g., major third and sweet) and the more common tone-colour synaesthesia in which each particular tone is linked to a specific colour (e.g., C and red).

One of the current theories of synaesthesia proposes that local crossactivation or disinhibition of feedback occurs because of increased connectivity between relevant brain areas. Based on diffusion tensor and T1-weighted magnetic resonance imaging we performed fractional anisotropy (FA) analysis, probabilistic fibre tractography, and voxel-based morphometry in the synaesthete E.S. compared with 17 professional musicians and 20 normal control subjects using voxel-wise *z*-score transformations.

We report increased FA and volumetric white (WM) and grey matter (GM) peculiarities in E.S.'s auditory and gustatory areas, hence explaining the interval-taste synaesthesia. Probabilistic fibre tractography revealed hyperconnectivity in bilateral perisylvian-insular regions in the synaesthete E.S. Differences in FA and volumetric WM and GM alterations in visual areas might represent the neuroarchitectural foundation of the tone-colour synaesthesia.

Still unknown are the causes of the structural alterations, although an X-chromosomal linked dominant trait has been suggested. Whether hyperconnectivity occurs due to a failure in neural pruning or even synaptic sprouting remains to be shown. Our findings might have implications for the understanding of multimodal integration and may encourage similar research into dysfunctional perceptual phenomenon such as hallucinations in schizophrenics or in Charles Bonnet syndrome.

Introduction

Synaesthesia is the involuntary physical experience of a cross-modal linkage, one common form of which is the additional sensation of seeing a colour (the concurrent perception) when hearing a tone (the inducing stimulus). The majority of synaesthesia types have colour as the concurrent perception (Rich and Mattingley, 2002), while concurrent perception of smell and taste types occur rarely (Ward and Simner, 2003; Simner and Ward, 2006; Pierce, 1907). But in a previous study, we described the case of the synaesthete E.S., a musician who experiences different tastes in response to hearing different music tone intervals (Beeli et al., 2005). This was the first case with this form of synaesthesia to be described in the literature. E.S. is 29 years of age, right-handed, and a female professional flute player. Whenever she hears a specific music tone interval she automatically experiences a taste on her tongue (e.g., minor second and sour; major third and sweet) that is consistently linked to that particular interval (Beeli et al., 2005). Besides this highly unusual interval-taste synaesthesia, she also reports the more common tone-colour synaesthesia in which each particular tone is linked to a specific colour (e.g., C and red; F sharp and violet). She has also absolute pitch perception. The cognitive mechanism and the neuroanatomical basis of these two forms as well as other forms of synaesthesia are still unknown. Several theories have been proposed to explain synaesthesia on the basis of neurophysiological and neuroanatomical constraints (Ramachandran and Hubbard, 2001; Grossenbacher and Lovelace, 2001; Smilek et al., 2001; Hubbard et al., 2005; Simner, 2007).

The present study draws on the theory that synaesthesia is rooted in local neurophysiological crossactivation (Baron-Cohen et al., 1993; Hubbard and Ramachandran, 2005), including disinhibition of feedback (Grossenbacher and Lovelace, 2001) and re-entrant of feedback (Smilek et al., 2001). To shed light on the possible neuroarchitectural basis of these neurophysiological mechanisms, we built on the suggestion of increased neuroanatomical connections among relevant brain areas (Ramachandran and Hubbard, 2001; Hubbard and

* Corresponding authors.
E-mail addresses: j.haenggi@psychologie.uzh.ch (J. Hänggi), l.jaencke@psychologie.uzh.ch (L. Jäncke).

1053-8119/$ – see front matter © 2008 Elsevier Inc. All rights reserved.
doi:10.1016/j.neuroimage.2008.07.018

Ramachandran, 2005) by examining the connectivity of white matter tracts as well as the volumetric properties of grey (GM) and white (WM) matter in brain structures responsible for the processing of the inducing stimulus and concurrent perception. With this approach we sought to verify our proposal that differences in the connectivity between relevant brain structures and volumetric properties of the brain structures involved might facilitate local crossactivation (Baron-Cohen et al., 1993; Hubbard and Ramachandran, 2005), disinhibition of feedback (Grossenbacher and Lovelace, 2001), or re-entrant of feedback (Smilek et al., 2001). Using diffusion tensor imaging (DTI) in grapheme-colour synaesthesia, other researchers have found higher fractional anisotropy (FA), a marker of increased coherent white matter tracts, in the right inferior temporal cortex, the left parietal cortex, and in bilateral frontal cortical areas in grapheme-colour synaesthetes compared with non-synaesthetes (Rouw and Scholte, 2007).

For interval-taste synaesthesia we expected morphological alterations in auditory areas (musical interval perception, audition) and in the insulae (taste perception, gustation) as well as in the fibre bundles between these areas. For tone-colour synaesthesia we expected morphological peculiarities in both the auditory areas (tone perception, audition) and lower- and higher-order visual areas (located in the ventral and dorsal visual processing stream), especially in the human colour processing areas (V4, V4α), sometimes also referred to as V8 (Hadjikhani et al., 1998) and in the fibre bundles between these areas. Furthermore, structural alterations in association with tone-colour synaesthesia were also expected in primary (V1, blobs) and secondary visual cortices (V2, thin stripes) because it has been shown that these areas are also colour sensitive (Tootell et al., 2004).

We report first findings on the neuroanatomical underpinnings of the interval-taste and tone-colour synaesthesia in the multiple synaesthete E.S. We used diffusion tensor imaging (DTI) to investigate the connectivity of white matter tracts by means of FA analysis and probabilistic fibre tractography on one hand and voxel-based morphometry (VBM) based on high-resolution volumetric 3D T1-weighted magnetic resonance imaging (MRI) to investigate GM and WM volumes on the other hand. Statistical analyses of the synaesthete's brain images, that is, FA and WM and GM volumes, were performed by voxel-wise *z*-score transformations in comparison with professional female musicians and female non-musicians in order to show hyperconnectivity and volumetric WM and GM differences. Since E.S. is also a musician having a command of absolute pitch we compared her brain measures with those of absolute pitch musicians.

We used professional musicians (including absolute pitch musicians) as control subjects because of the known modulatory impact of intensive musical training on auditory and sensorimotor brain areas at a structural level, at least in keyboard and string players (Bengtsson et al., 2005; Keenan et al., 2001; Gaser and Schlaug, 2003; Schlaug et al., 1995; Hutchinson et al., 2003) and because of absolute pitch (Wu et al., 2008; Gaab et al., 2006; Hamilton et al., 2004).

Methods

Behavioural data

We compared the brain of the synaesthete E.S. with brains of 20 normal control females as well as with brains of 17 professional female musicians, 10 of whom had absolute and 7 relative pitch perception. These subjects were approximately matched to the synaesthete E.S. with respect to age, education, and handedness. Professional musicians were participants in an ongoing study on absolute pitch perception and musical abilities at our institution. This sample is balanced with respect to keyboard and string players. Absolute pitch perception performance was evaluated by one of the authors (M.S.O.) as described in the Supplementary data online. For the evaluation of the music interval-taste synaesthesia of E.S. (see Beeli et al., 2005). The tone-colour synaesthesia was evaluated by one of the authors (G.B.) as described in the Supplementary data online (pitch-colour Stroop task and Fig. S1). The subjects reported no past or current psychiatric, neurological, and neuropsychological problems and denied taking illegal drugs or medication. The local ethics committee approved the study and written informed consent was obtained from all participants as well as the permission from the synaesthete to publish her initials.

MRI data acquisition

Magnetic resonance imaging (MRI) scans were acquired on two different MR systems. The synaesthete was scanned on both systems. The normal control subjects were scanned on one system and the professional musicians on the other system. MR images of normal control subjects were acquired on a 3.0 T Philips Intera whole-body scanner (Philips Medical Systems, Best, The Netherlands) equipped with a transmit-receive body coil and a commercial eight-element sensitivity encoding (SENSE) head coil array. MR images of the professional musicians were acquired on a 3.0 T General Electrics Signa Excite II whole-body MR system (GE Healthcare, Milwaukee, U.S.A) using a standard 8-channel head coil array.

Diffusion tensor MRI scans

Normal control subjects. Diffusion-weighted spin-echo echo-planar (EPI) sequence scans were obtained with a measured spatial resolution of 2.08×2.13×2.0 mm^3 (acquisition matrix 96×96 pixels, 50 slices) and a reconstructed resolution of 1.56×1.56×2.0 mm^3 (reconstructed matrix 128×128 pixels, 50 slices). Further imaging parameters were: field of view FOV=200×200 mm^2, echo-time TE=50 ms, repetition-time TR=10166 ms, flip-angle FA=90°, and SENSE factor R=2.1. Diffusion was measured in 15 non-collinear directions followed by a non-diffusion-weighted volume (reference volume). Total acquisition time was about 16 min.

Professional musicians. Diffusion-weighted axial imaging was performed in accordance with an imaging plane parallel to the antero-posterior commissural line. We sampled the diffusion tensor by repeating a diffusion-weighted single-shot spin-echo echo-planar (EPI) sequence along 21 different geometric directions. Diffusion sensitization was achieved with 2 balanced diffusion gradients centred on the 180° radio-frequency pulse. An effective b-value of 1000 s/mm^2 was used for each of the 21 diffusion-encoding directions. Three measurements were performed without diffusion weighting (b 0 of 0 s/mm^2) at the beginning of the sequence. Scan parameters were TR=8000 ms; TE=91 ms; matrix size=128×128; and FOV=240×240 mm. A total of 42 contiguous 3-mm-thick axial sections were acquired. Total acquisition time was about 6 min.

T1-weighted MRI scans

Normal control subjects. A volumetric 3D T1-weighted gradient echo sequence (TFE, turbo field echo) scan was obtained with a measured spatial resolution of 1×1×1.5 mm^3 (acquisition matrix 224×224 pixels, 180 slices) and a reconstructed resolution of 0.86×0.86×0.75 mm^3 (reconstructed matrix 256×256 pixels, 180 slices). Further imaging parameters were: field of view FOV=220×220 mm^2, echo-time TE=2.3 ms, repetition-time TR=20 ms, and flip-angle FA=20°. Total acquisition time was about 8 min.

Professional musicians. A volumetric 3D T1-weighted fast spoiled gradient echo (FSPGR) sequence scan was obtained with a measured and reconstructed resolution of 0.94×0.94×1.0 mm^3 (matrix 256×256

pixels, 172 slices). Further imaging parameters were: field of view FOV = 220 × 220 mm^2, echo-time TE = 2.1 ms, repetition-time TR = 9.3 ms, and flip-angle FA = 20°. Total acquisition time was about 7 min.

MRI data preprocessing and statistical analyses

MRI data preprocessing as well as statistical comparisons between the synaesthete and the normal control subjects on one hand and between the synaesthete and the professional musicians on the other hand was identical, i.e., there were no differences due to preprocessing and statistics between the data acquired on the different MR systems.

In order to compare the brain of a single subject with the brains of a group, we constructed voxel-wise *z*-score images for that single subject brain. Because canonical a priori maps were derived from male and female brains and our sample is comprised of females only, we used customised a priori maps for spatial normalisation and tissue class segmentation in the preprocessing of the T1-weighted MR scans. These customised a priori maps were derived from T1-weighted MR images of 125 healthy control females (age: mean/sd: 25.6/6.6 years) scanned on the same 3 T Philips Intera scanner with the same pulse sequence as used for the normal control subjects. This template was used for spatial normalisation and tissue class segmentation of the T1-weighted data derived from both MR systems. For spatial normalisation of the diffusion-weighted MR data we used the canonical 152 T1-weighted reference brain template from the MNI (Montreal Neurological Institute).

Analysis of fractional anisotropy (FA)

We applied parts of the processing stream of Tract-Based Spatial Statistics (TBSS) (Smith et al., 2006), but we left the pipeline before skeletonization. Preprocessing steps were performed with the diffusion toolbox (FDT) (Behrens et al., 2003a,b). FDT and TBSS are part of the software library (FSL, Version 3.3 and 4.0) (Smith et al., 2004) and are implemented in the functional magnetic resonance imaging of the brain (FMRIB) software library package (http://www.fmrib.ox.ac.uk/fsl/). These tools were used to create fractional anisotropy (FA) maps. The steps were realised in the following order: 1) eddy current and motion correction were applied using the EDDYCORRECT tool. 2) Tensors were fitted to the data using the DTIFIT tool. 3) Linear and non-linear registration of all FA data into standard space was applied using TBSS. 4) FA images were smoothed with a Gaussian kernel of FWHM = 12 mm. 5) Smoothed FA images of the control group were averaged and a standard deviation image was computed. 6) The FA mean image and the FA image of the synaesthete were masked with a threshold of 0.2 to exclude voxels with low FA values. 7) Theses images were masked with each other to exclude voxels that are not common in both images. 8) *z*-score maps for the synaesthetic subject were computed by voxel-wise subtracting the group FA mean image from the synaesthete FA image and dividing by the standard deviation image. 9) These fractional anisotropy *z*-score images were thresholded with a height threshold of $z = \pm 3.1$ ($p < 0.001$, uncorrected for multiple comparisons) and with an extent threshold of $k = 50$ voxels (equals 50 mm^3). Steps 4–9 were performed using SPM5. In the face of strong a priori hypotheses with respect to the expected locations of FA differences, multiple comparisons correction procedures are too conservative and hence inappropriate (see discussion).

Analyses of grey (GM) and white matter (WM) volumes

Here we applied the preprocessing stream of voxel-based morphometry (VBM) (Ashburner and Friston, 2000) implemented in the VBM5 toolbox (http://dbm.neuro.uni-jena.de/vbm/) for the statistical parametric mapping (SPM5) software (http://www.fil.ion.ucl.ac.uk/spm/). The following steps were realised: 1) the coordinate origin was manually set on the anterior commissure. 2) Intensity inhomogeneity (bias field) correction, tissue class segmentation, and spatial normalisation (affine and warping) were performed using the unified segmentation approach (Ashburner and Friston, 2005). 3) To investigate absolute volumes, Jacobian modulation was applied to the deformation fields in order to control for the volume changes introduced by the spatial normalisation procedure. 4) To enhance tissue class segmentation, Hidden Markov Random Field (HMRF) modulation was applied (Cuadra et al., 2005; http://dbm.neuro.uni-jena.de/vbm/) to introduce local constraints for the tissue classifier. 5) In order to adjust for total tissue volumes GM and WM segments were divided by the total GM and WM volume, respectively. 6) GM and WM images were smoothed with a Gaussian kernel of FWHM = 12 mm. 7) Smoothed GM and WM images of the control group were averaged separately and GM and WM standard deviation images were computed. 8) The GM and WM mean images and the GM and WM images of the synaesthete were masked with a threshold of 0.2 to exclude voxels with low tissue type probabilities. 9) Theses images were masked with each other to exclude voxels that are not common in both images. 10) *z*-score maps for the synaesthetic subject were voxel-wise computed by subtracting the group mean image from the synaesthete image and dividing by the standard deviation image of the group. 11) These *z*-score images were thresholded with a height threshold of $z = \pm 3.1$ ($p < 0.001$, uncorrected for multiple comparisons) and with an extent threshold of $k = 50$ voxels for GM and WM volumes. In the face of strong a priori hypotheses with respect to the expected locations of GM and WM volume differences, multiple comparisons correction procedures are too conservative and hence inappropriate (see discussion).

Probabilistic fibre tractography

We also performed fibre tractography (Behrens et al., 2003a,b, 2007) in the synaesthete E.S. and in the 10 professional female musicians with absolute pitch perception. Whereas FA analysis only delivers information about tract orientation in a particular region, probabilistic tractography shows additionally which areas are hyper-connected with each other. Probabilistic fibre tractography was applied to the already preprocessed DTI data with 21 non-collinear diffusion gradient directions derived from the FA analysis using the FDT tool (see above). Briefly, FDT repetitively samples from the distributions on voxel-wise principal diffusion directions, each time computing a streamline through these local samples to generate a probabilistic streamline or a sample from the distribution on the location of the true streamline. By taking many such samples FDT is able to build up the posterior distribution on the streamline location or the "*connectivity distribution*" (Behrens et al., 2003a; http://www.fmrib.ox.ac.uk/fsl/fdt/fdt_probtrackx.html). The local diffusion directions were calculated using the BEDPOSTX tool allowing modelling multiple fibre orientations per voxel. Tractographic analyses were performed with the PROBTRACX tool using a multiple regions of interest (ROIs) approach. We focussed on three neighbouring ROIs in each hemisphere: the insula, the Heschl's gyrus, and the planum temporale, regions in which we found large differences in FA between the synaesthete E.S. and the two different control groups. In such a multiple ROIs approach only tracts that pass through all ROIs, i.e., through the insula, the Heschl's gyrus, and the planum temporale, were retained. The connectivity distributions were visualised and the number of tract voxels as well as connectivity distributions values was computed.

Results

Refer to Supplementary data (Table S1), available online, for the demographic characteristics of the synaesthete E.S., the 20 normal control subjects, and the 17 professional musicians. Local differences in fractional anisotropy (FA) between the synaesthete's brain and the brains of the normal control subjects (Figs. 1a–c) on one hand and between the synaesthete's brain and the brains of the professional

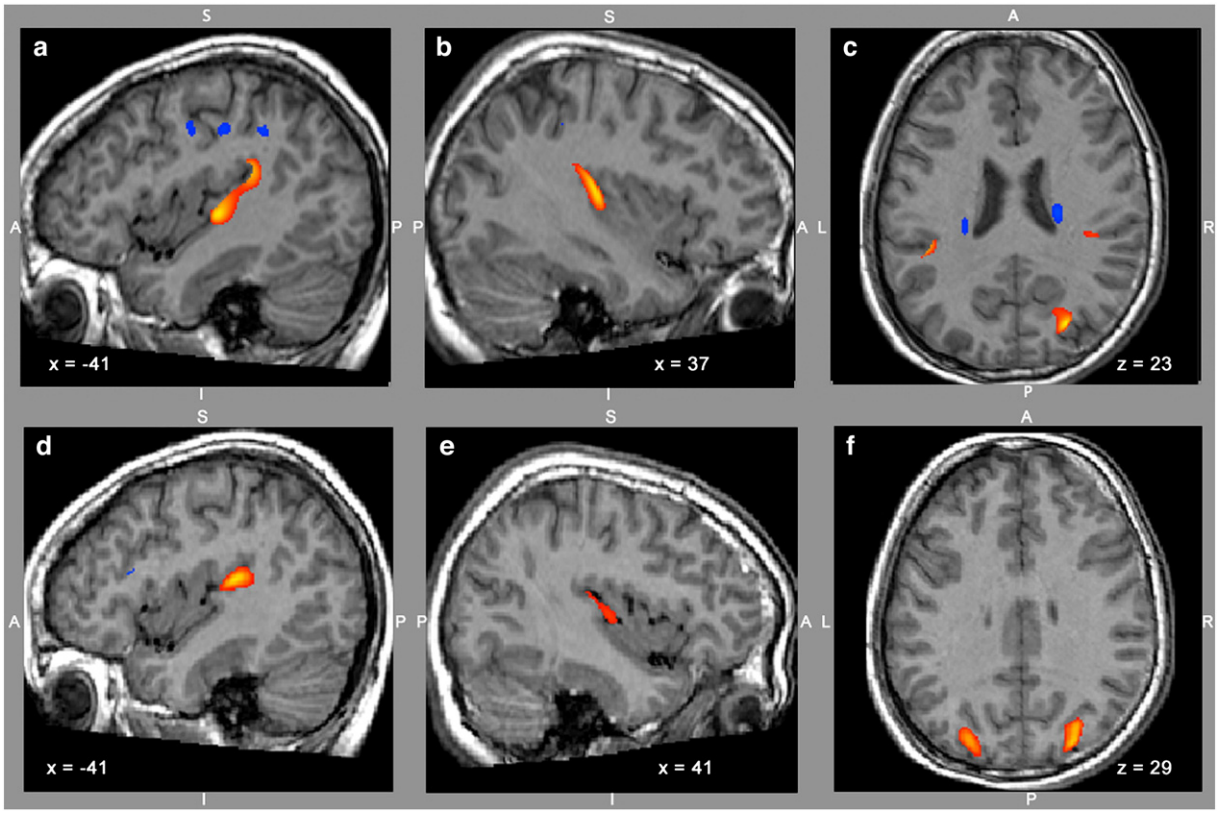

Fig. 1. Increased (red-yellow, $z>3.1$, $p<0.001$) and decreased (blue-lightblue, $z<-3.1$, $p<0.001$) fractional anisotropy (FA) in the brain of the synaesthete E.S. compared with 20 normal control subjects (a–c) and 17 professional musicians (d–f). Increased FA was found in the left planum temporale/Heschl's gyrus/insula (a, d), right planum temporale/Heschl's gyrus (b, e), and in both lateral superior occipital cortices (c, f). For further clusters highlighted in the figure see Tables 1 and 2. The FA *z*-score maps are superimposed on the structural MR image of the synaesthete E.S.

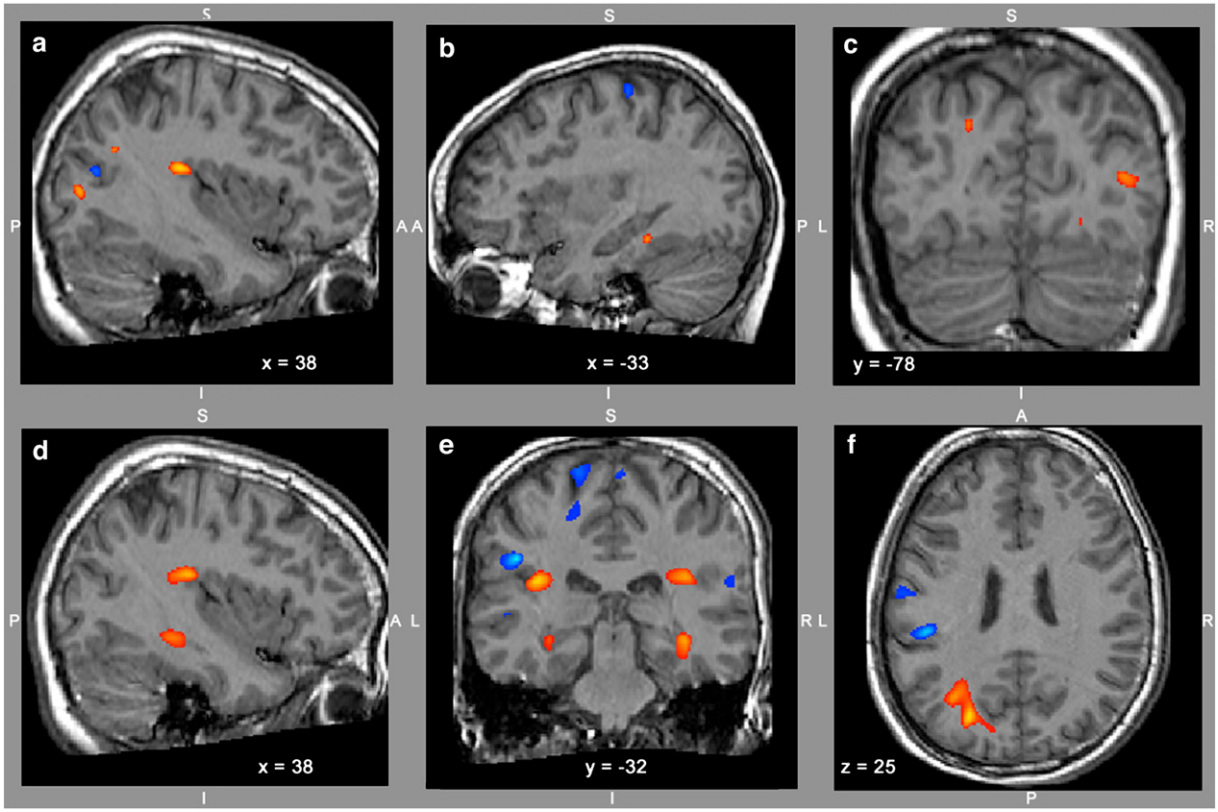

Fig. 2. Increased (red-yellow, $z>3.1$, $p<0.001$) and decreased (blue-lightblue, $z<-3.1$, $p<0.001$) white matter (WM) volumes in the brain of the synaesthete E.S. compared with 20 normal control subjects (a–c) and 17 professional musicians (d–f). Increased WM volume was found in the right planum temporale/Heschl's gyrus (a, d, e), left planum temporale and both hippocampi (e), in occipital regions (c), and in the left optic radiation (f). For further clusters highlighted in the figure see Tables 1 and 2. The WM volumes *z*-score maps are superimposed on the structural MR image of the synaesthete E.S.

musicians (Figs. 1d–f) on the other hand are shown in Fig. 1. Local white matter (WM) and grey matter (GM) volume differences between the synaesthete E.S. and the normal control subjects are shown in Figs. 2a–c and 3a–c, respectively, whereas the WM and GM volume differences between the synaesthete E.S. and the professional musicians are presented in Figs. 2d–f and 3d–f, respectively. Summaries of all structural brain differences in the brain of E.S. are presented in Table 1 for the comparison with the normal control females and in Table 2 for the comparison with the professional female musicians. Results of the probabilistic tractography are visualised in Fig. 5 and quantified in Fig. 6.

For WM connectivity increased FA (red-yellow, $z>3.1$, $p<0.001$) was found in the synaesthete's brain compared with the normal control subjects in a large cluster comprised by the left planum polare/Heschl's gyrus/insula/planum temporale/parietal operculum (Fig. 1a), in the right insula/Heschl's gyrus (Fig. 1b), and in the right superior occipital gyrus (Fig. 1c). Decreased FA (blue-lightblue, $z<-3.1$, $p<0.001$) was found in the left supramarginal gyrus, in the left post- and precentral gyrus (Fig. 1a), and in the left and right corticospinal tract (Fig. 1c).

In comparison with professional musicians the above FA findings were replicated. Increased FA in the brain of E.S. was found in the left planum temporale/Heschl's gyrus (Fig. 1d), in the right Heschl's gyrus/insula (Fig. 1e), and in the left and right lateral occipital cortex (Fig. 1f), although these clusters were not as large as the clusters found in that regions in comparison with the normal control subjects. Decreased FA values in E.S. were evident in the left internal capsule, left postcentral gyrus, right precentral gyrus, left corticospinal tract, left posterior thalamic radiation, both anterior intraparietal sulci, and in the right pallidum.

Increased WM volumes (red-yellow, $z>3.1$, $p<0.001$) were evident in the synaesthete's brain compared with normal control subjects in the right Heschl's gyrus/planum temporale/parietal operculum (Fig. 2a), right middle occipital gyrus (Figs. 2a, c), left fusiform gyrus (Fig. 2b), and in the left superior occipital gyrus. Decreased WM volumes (blue-lightblue, $z<-3.1$, $p<0.001$) were found in the right middle temporo-occipital gyrus (Fig. 2a) and in the left pre-/postcentral gyrus (Fig. 2b).

Compared with professional musicians increased WM volumes in E.S. were found in her right (Fig. 2d) and left planum temporale (Fig. 2e), right hippocampus/optic radiation and in the left cuneus/optic radiation (Fig. 2f). Decreased WM volumes were evident in the right planum temporale, left superior temporal gyrus, left parietal operculum, as well as in pre- and postcentral gyri.

In the case of GM volume, we found increased GM volumes (red-yellow, $z>3.1$, $p<0.001$) in the synaesthete's brain compared with control subjects in the right middle and inferior occipital gyrus (Figs. 3a, b), right middle and inferior temporo-occipital gyrus, left middle occipital gyrus, right middle temporal gyrus, and left thalamus (Fig. 3b). Decreased GM volumes (blue-lightblue, $z<-3.1$, $p<0.001$) were found in the left superior temporal gyrus (Figs. 3a, b) and in the left insula (Fig. 3c).

In contrast to professional musicians, increased GM volumes were evident in her left lateral occipital cortex (Fig. 3f), right lateral occipital cortex, in both thalami, as well as in her bilateral occipital poles (V2). Decreased GM volumes were evident in her left Heschl's gyrus/planum temporale/insula (Fig. 3d), right Heschl's gyrus (Fig. 3e), right planum temporale, right anterior and posterior superior temporal gyrus, right temporo-occipital cortex, and in both superior parietal lobules.

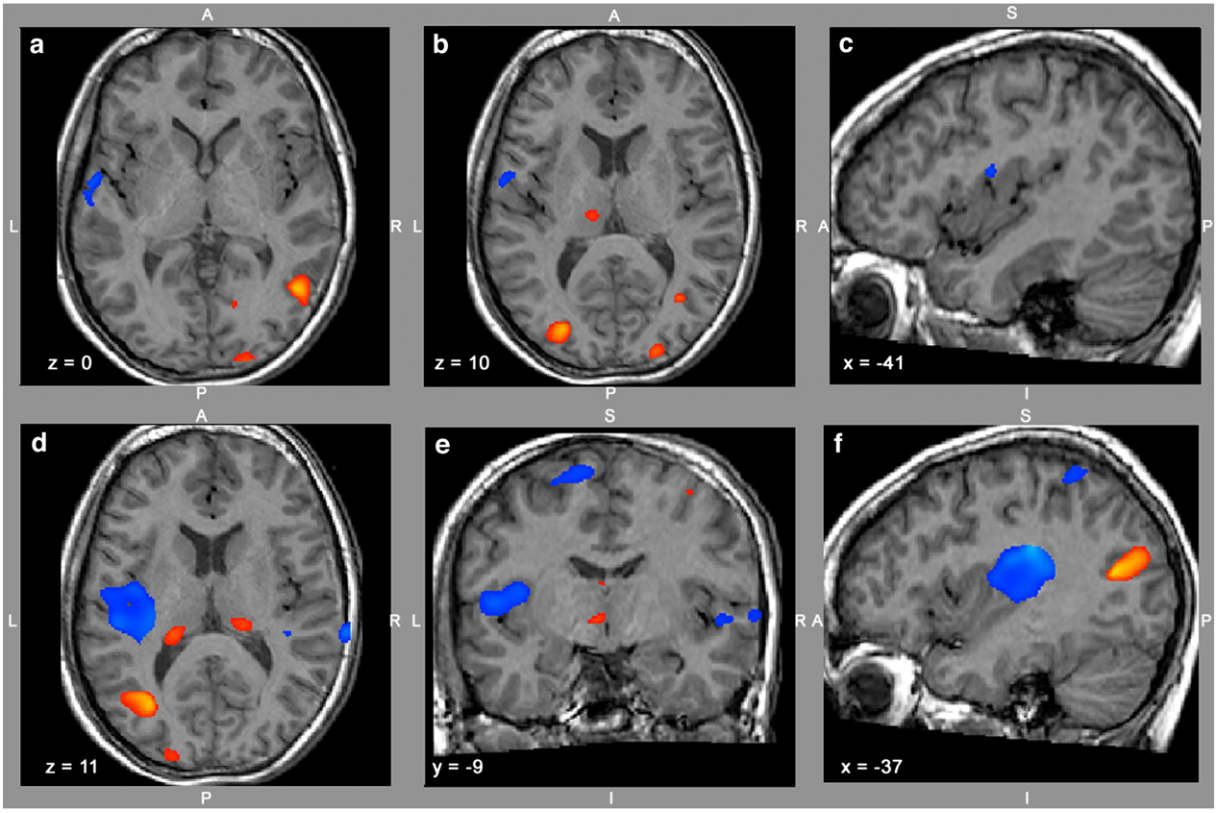

Fig. 3. Increased (red-yellow, $z>3.1$, $p<0.001$) and decreased (blue-lightblue, $z<-3.1$, $p<0.001$) grey matter (GM) volumes in the brain of the synaesthete E.S. compared with 20 normal control subjects (a–c) and 17 professional musicians (d–f). Increased GM volume was evident in occipital, temporo-occipital, and thalamic regions (a, b, d, f). Decreased GM volume was found in the left superior temporal gyrus and insula (a–c), left Heschl's gyrus/planum temporale/insula (d–f), and in the right superior temporal gyrus, Heschl's gyrus, and planum temporale (d, e). For further clusters highlighted in the figure see Tables 1 and 2. The GM volumes z-score maps are superimposed on the structural MR image of the synaesthete E.S.

Table 1
Summary of fractional anisotropy and volumetric brain differences between the synaesthete E.S. and 20 normal control subjects

Synaesthete E.S.>normal control subjects	Cluster size mm^3	MNI coordinates			Mean *z*-score	S.D.	Max.
		x	*y*	*z*			
Fractional anisotropy							
Left planum polare/Heschl's gyrus/insula/planum temporale/parietal operculum (superior and inferior longitudinal fasciculus) (Figs. 1a, c)	1352	−41	−28	8	3.57	0.372	4.71
Right insula/Heschl's gyrus (Figs. 1b, c)	775	37	−24	13	3.60	0.385	4.68
Right superior occipital gyrus (Fig. 1c)	550	25	−74	23	3.56	0.391	4.77
Right middle cingulate gyrus (cingulum)	615	5	8	37	3.35	0.186	3.94
Right anterior cingulate gyrus	200	7	36	−5	3.49	0.299	4.28
Right middle cerebellar peduncle	807	20	−43	−32	3.32	0.164	3.80
Left middle cerebellar peduncle	393	−19	−41	−29	3.66	0.411	4.69
White matter volume							
Right Heschl's gyrus/planum temporale/parietal operculum (Fig. 2a)	357	39	−30	17	3.40	0.204	3.87
Left fusiform gyrus (Fig. 2b)	68	−32	−38	−17	3.25	0.102	3.49
Right middle occipital gyrus (Figs. 2a, c)	186	39	−77	6	3.27	0.118	3.56
Left superior occipital gyrus (Fig. 2c)	65	−19	−79	26	3.23	0.087	3.42
Right precentral/superior frontal gyrus	108	29	−8	59	3.32	0.148	3.66
Left brainstem	58	−13	−16	−23	3.17	0.046	3.26
Grey matter volume							
Right middle and inferior occipital gyrus (Figs. 3a, b)	1410	23	−97	1	3.41	0.242	4.29
Left middle occipital gyrus (Fig. 3b)	865	−29	−84	9	3.68	0.427	4.81
Left inferior occipital gyrus	74	−28	−91	−8	3.22	0.083	3.39
Right middle and inferior temporo-occipital gyrus (Fig. 3a)	1752	50	−63	−3	3.69	0.499	5.34
Right middle temporal gyrus (Fig. 3b)	635	37	−68	15	3.88	0.628	5.71
Right inferior temporal gyrus	158	39	−66	−7	3.29	0.128	3.59
Left thalamus (Fig. 3b)	290	−12	−24	7	3.29	0.136	3.63
Right medial frontal gyrus	133	20	1	52	3.43	0.219	3.94
Left precentral gyrus	60	−35	5	41	3.31	0.134	3.61
Synaesthete E.S.<normal control subjects	**Cluster size mm^3**	**MNI coordinates**			**Mean *z*-score**	**S.D.**	**Min.**
		x	*y*	*z*			
Fractional anisotropy							
Right superior parietal lobule	533	31	−41	42	−3.62	0.403	−4.75
Left supramarginal gyrus (Fig. 1a)	149	−40	−41	38	−3.23	0.092	−3.46
Left middle frontal gyrus	379	−27	50	1	−3.52	0.367	−4.70
Right superior frontal gyrus	160	23	2	55	−3.27	0.119	−3.53
Left postcentral gyrus	638	−30	−35	54	−3.33	0.164	−3.77
Left postcentral gyrus (Fig. 1a)	157	−43	−23	39	−3.23	0.092	−3.43
Left precentral gyrus	187	−24	−20	61	−3.35	0.169	−3.73
Left precentral gyrus (Fig. 1a)	93	−43	−8	40	−3.22	0.089	−3.42
Right precentral gyrus	104	33	−24	57	−3.19	0.079	−3.41
Right precentral gyrus (superior longitudinal fasciculus)	385	41	−7	36	−3.40	0.207	−3.88
Right corticospinal tract (Fig. 1c)	269	22	−19	23	−3.30	0.145	−3.66
Left corticospinal tract (Fig. 1c)	138	−25	−26	23	−3.18	0.062	−3.33
Pons	55	−2	−17	−32	−3.19	0.072	−3.34
Genu of corpus callosum	1900	6	22	5	−4.05	0.759	−6.27
White matter volume							
Right middle temporo-occipital gyrus (Fig. 2a)	88	39	−69	16	−3.37	0.184	−3.80
Right superior parietal lobule	62	27	−46	50	−3.12	0.017	−3.16
Right superior frontal gyrus	66	20	3	59	−3.16	0.040	−3.24
Right precentral gyrus	55	27	−25	61	−3.17	0.046	−3.26
Left superior parietal lobule/postcentral gyrus	1398	−22	−47	57	−3.95	0.627	−5.66
Left precentral/postcentral gyrus (Fig. 2b)	871	−28	−26	60	−3.69	0.434	−4.99
Grey matter volume							
Left superior temporal gyrus (Figs. 3a, b)	876	−58	−5	2	−3.43	0.279	−4.30
Left insula (Fig. 3c)	84	−40	−4	16	−3.31	0.151	−3.66

Note. For labelling of fractional anisotropy and white matter volume clusters the nearest grey matter label was used because no exhaustive white matter atlas is available as yet. Available white matter labels are indicated in brackets. *Abbreviations*: S.D., standard deviation; Max., maximum; Min., minimum; MNI, Montreal Neurological Institute; Fig., figure.

Additional brain areas (figures not shown) with FA and volumetric WM and GM differences in the synaesthete E.S. are shown in Table 1 in comparison with the normal control subjects and in Table 2 in comparison with the professional musicians. Most of these areas were located in occipital, temporo-occipital, and parietal regions, and in both pre- and postcentral gyri (primary motor and somatosensory areas) as well as in both thalami.

Clusters of significant increased FA (as shown in Fig. 1) and increased WM volumes (as shown in Fig. 2) in the brain of the synaesthete E.S. were collated in Fig. 4 in order to show the spatial relations between the differences in FA and WM volumes on one hand and between the comparison with normal control subjects and professional musicians on the other hand.

Probabilistic tractographs revealed hyperconnectivity in bilateral perisylvian-insular regions in the synaesthete E.S. (red-yellow tracts) compared with the average tractograph of the 10 female professional musicians with absolute pitch (blue-lightblue tracts) (Fig. 5). In the left hemisphere of E.S. there is one tract directed laterally to the left planum temporale and one tract directed inferior-medially toward the left thalamus (Fig. 5a), the later one most probably represents parts of the optic and acoustic radiations. In her right hemisphere the hyperconnected tract is directed laterally to the right planum

Table 2
Summary of fractional anisotropy and volumetric brain differences between the synaesthete E.S. and 17 professional musicians

Synaesthete E.S.>professional musicians	Cluster size mm^3	MNI coordinates			Mean *z*-score	S.D.	Max.
		x	*y*	*z*			
Fractional anisotropy							
Left planum temporale/Heschl's gyrus (Fig. 1d)	855	−42	−32	13	3.79	0.563	5.63
Right Heschl's gyrus/insula (Fig. 1e)	225	41	−17	7	3.22	0.095	3.47
Left lateral occipital cortex (Fig. 1f)	1493	−25	−83	32	3.63	0.366	5.00
Right lateral occipital cortex (Fig. 1f)	1420	27	−78	28	3.75	0.503	5.28
Right middle temporal gyrus, temporo-occipital part	97	66	−44	9	3.34	0.166	3.74
Right superior frontal gyrus/premotor cortex	109	20	1	63	3.29	0.133	3.59
Left cerebellum, uvula of vermis	2443	−2	−65	−34	3.65	0.404	4.87
White matter volume							
Right planum temporale (Fig. 2d)	932	35	−30	19	3.66	0.414	4.84
Left planum temporale (Fig. 2e)	879	−36	−32	17	3.78	0.493	5.11
Right hippocampus/optic radiation (Fig. 2e)	909	35	−34	−12	3.63	0.391	4.61
Left optic radiation/cuneus (Fig. 2f)	2198	−23	−72	25	3.52	0.398	5.17
Right intracalcarine cortex, V1	54	6	−88	6	3.30	0.158	3.68
Right corticospinal tract	111	11	−10	−23	3.34	0.167	3.73
Left hippocampus (Fig. 2e)	329	−32	−34	−10	3.30	0.159	3.79
Left superior frontal gyrus	81	−24	21	54	3.29	0.123	3.55
Left cerebellum	626	−19	−65	−49	3.76	0.510	5.39
Grey matter volume							
Left lateral occipital cortex (Fig. 3f)	2510	−37	−72	15	4.19	0.853	6.73
Left occipital pole, V2	234	−20	−97	10	3.26	0.116	3.55
Right lateral occipital cortex	604	51	−78	−7	3.48	0.255	4.02
Right occipital pole, V2	238	26	−91	−7	3.21	0.073	3.41
Left thalamus	519	−19	−34	9	3.44	0.243	4.07
Left thalamus	222	−1	−15	14	3.26	0.117	3.55
Left thalamus	649	−2	−4	−3	3.51	0.292	4.26
Right thalamus	314	16	−28	11	3.33	0.152	3.69
Left middle temporal gyrus, posterior part	127	−63	−39	−9	3.25	0.109	3.51
Right inferior temporal gyrus, posterior part	74	45	−34	−21	3.38	0.201	3.87
Left subcallosal cortex	313	−10	26	−14	3.22	0.085	3.42
Right nucleus accumbens	254	9	20	−7	3.28	0.124	3.59
Synaesthete E.S.<professional musicians	**Cluster size mm^3**	**MNI coordinates**			**Mean *z*-score**	**S.D.**	**Min.**
		x	*y*	*z*			
Fractional anisotropy							
Left internal capsula	1458	−25	−24	4	−3.68	0.446	−4.87
Left posterior thalamic radiation	255	−34	−55	7	−3.50	0.284	−4.22
Left anterior intraparietal sulcus	76	−19	−61	37	−3.26	0.124	−3.54
Right anterior intraparietal sulcus	66	24	−53	36	−3.19	0.061	−3.33
Right lateral occipital gyrus	72	19	−63	51	−3.22	0.082	−3.39
Right pallidum	143	22	−12	−6	−3.39	0.234	−3.99
Left postcentral gyrus	354	−25	−36	62	−3.31	0.140	−3.64
Left precentral gyrus, corticospinal tract	86	−45	−5	38	−3.30	0.146	−3.63
Right precentral gyrus	105	26	−18	60	−3.22	0.072	−3.38
Left inferior frontal gyrus, triangular part	87	−39	23	17	−3.34	0.156	−3.69
Right frontal pole	57	27	45	22	−3.22	0.082	−3.40
White matter volume							
Right planum temporale	89	58	−32	17	−3.26	0.102	−3.49
Left superior temporal gyrus	92	−52	−30	1	−3.38	0.196	−3.84
Left parietal operculum	667	−48	−30	26	−4.27	0.106	−8.02
Left superior parietal lobule	380	−24	−43	43	−3.33	0.168	−3.78
Left precentral gyrus	1614	−17	−29	59	−3.45	0.305	−4.61
Right precentral gyrus	127	4	−30	67	−3.41	0.225	−3.97
Left postcentral gyrus	566	−54	−12	27	−3.39	0.202	−3.93
Left superior frontal gyrus	599	−18	2	58	−3.58	0.324	−4.32
Grey matter volume							
Left Heschl's gyrus/planum temporale/insula (Fig. 3d)	12087	−43	−20	11	−3.86	0.648	−8.22
Right Heschl's gyrus (Fig. 3e)	225	52	−9	−2	−3.27	0.128	−3.59
Right anterior superior temporal gyrus	833	65	−4	−6	−3.49	0.298	−4.53
Right posterior superior temporal gyrus	641	70	−34	15	−3.97	0.643	−5.60
Right planum temporale	64	40	−31	9	−3.29	0.146	−3.65
Right middle temporal gyrus, temporo-occipital part	51	70	−41	1	−3.19	0.070	−3.35
Left superior parietal lobule	1129	−32	−50	59	−3.63	0.390	−4.73
Right superior parietal lobule	203	15	−52	68	−3.33	0.156	−3.69
Left superior frontal gyrus, premotor cortex	1966	−15	−9	64	−3.55	0.366	−5.03
Left superior frontal gyrus, premotor cortex	259	−19	6	66	−3.35	0.180	−3.80
Left precentral gyrus	221	−23	−28	68	−3.25	0.107	−3.51
Left postcentral gyrus	228	−51	−31	41	−3.44	0.169	−3.75
Left posterior cingulate gyrus	923	−13	−28	39	−3.54	0.341	−4.53

Note. For labelling of fractional anisotropy and white matter volume clusters the nearest grey matter label was used because no exhaustive white matter atlas is available as yet. Available white matter labels are indicated in brackets. *Abbreviations*: S.D., standard deviation; Max., maximum; Min., minimum; MNI, Montreal Neurological Institute; Fig., figure.

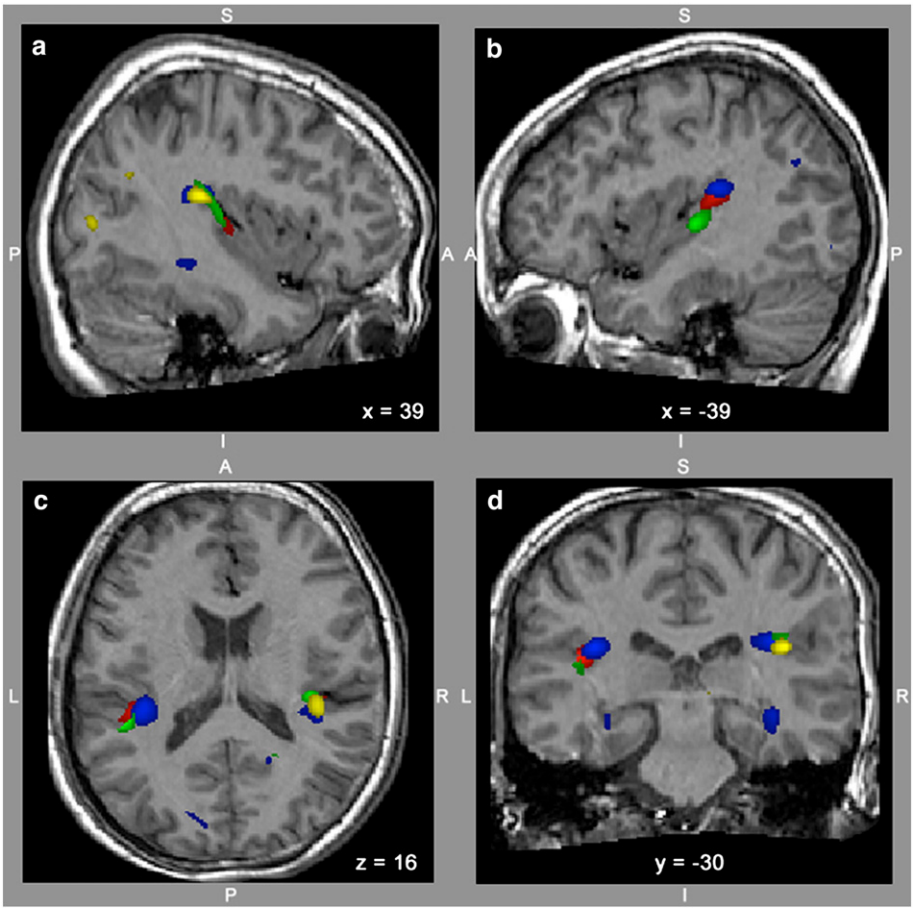

Fig. 4. Clusters of significant increased fractional anisotropy (FA) (as shown in Fig. 1) and increased white matter (WM) volumes (as shown in Fig. 2) in the brain of the synaesthete E.S. compared with 20 normal control subjects (FA in green; WM volumes in yellow) and 17 professional musicians (FA in red; WM volumes in blue). Shown are a right (a) and a left sagittal plane (b) through the perisylvian cortex and the insular region as well as the corresponding axial (c) and coronal (d) planes. The *z*-score maps are superimposed on the structural MR image of the synaesthete E.S.

temporale (Fig. 5b). Fig. 5a shows the coronal slice ($y=-30$) with the largest tractographic difference in the left–right direction in the left hemispheric tractograph. Fig. 5b shows the transversal slice ($z=14$) with the largest tract difference in the left–right direction in the right hemispheric tractograph.

We further quantified the probabilistic fibre tractographs by computing the number of suprathreshold voxels and the mean probabilistic connectivity distribution across all voxels that are part of the tractographs (Fig. 6). The number of suprathreshold voxels in the tractographs of both hemispheres is larger in the synaesthete E.S. than in the average tractograph of the 10 musicians with absolute pitch. Transformations of these measures into *z*-scores for the synaesthete E.S. revealed only statistical trends toward significance: $z=1.39$ and $z=1.20$ corresponding to probabilities of $p=0.082$ and

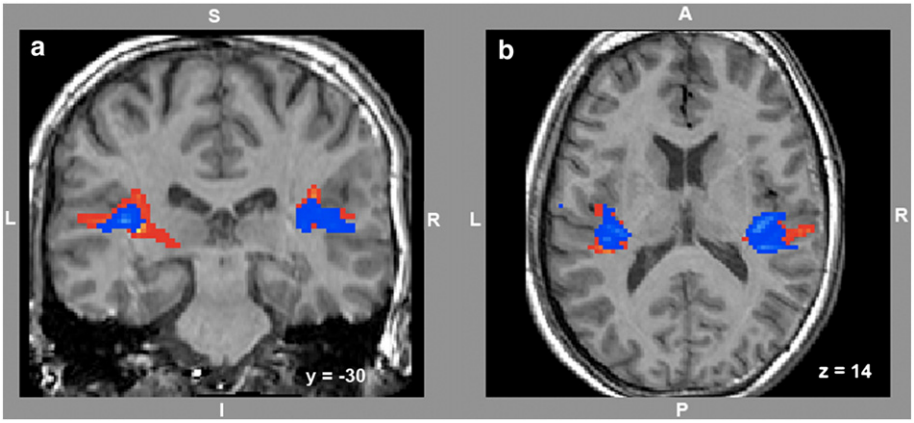

Fig. 5. Probabilistic fibre tractographs of the synaesthete E.S. (red-yellow) and the average tractographs of the 10 professional musicians with absolute pitch (blue-lightblue). We used a multiple regions of interest (ROI) approach to invoke tractography. ROIs were placed bilaterally in the insula, the Heschl's gyrus, and the planum temporale, hence only tracts that pass trough all three ROIs were retained. Panel a shows the coronal slice with the largest tractographic difference in the left–right direction in the left tractograph. Panel b shows the transversal slice with the largest tract difference in the left–right direction in the right tractograph. Tractographs are superimposed on the structural MR image of the synaesthete E.S.

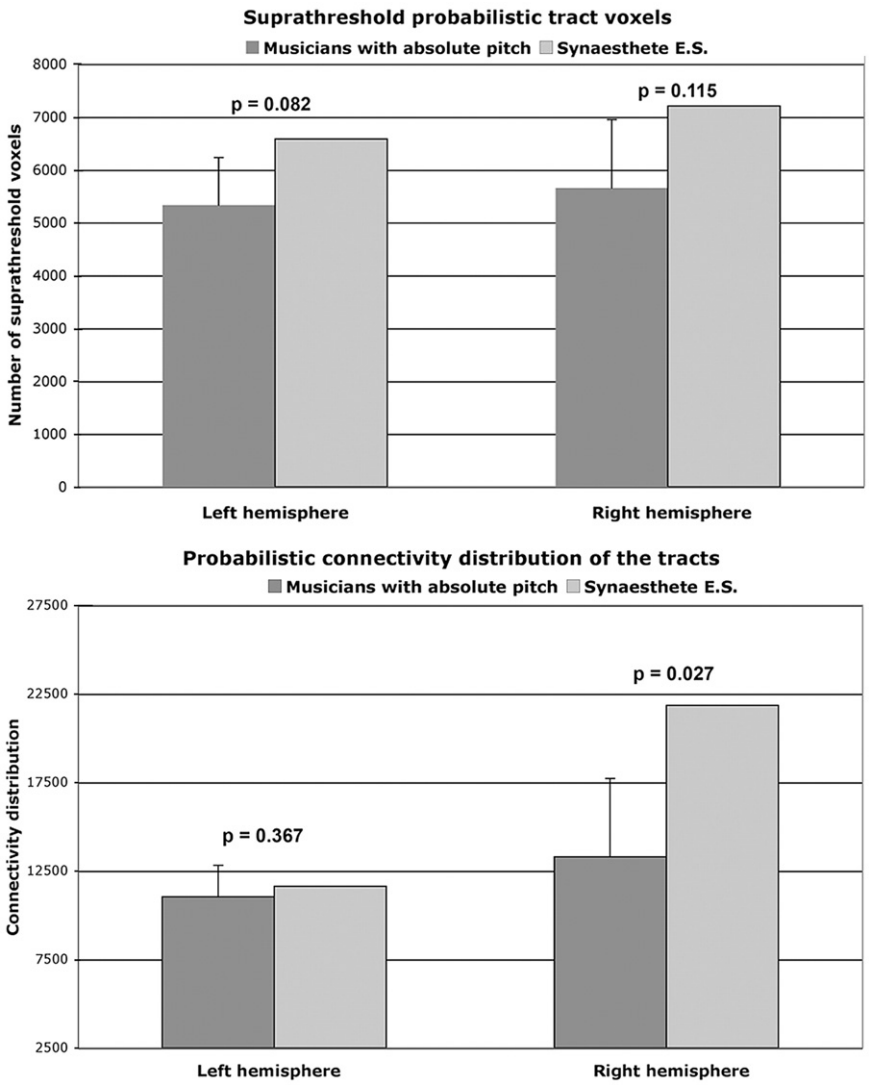

Fig. 6. Shown are the numbers of suprathreshold probabilistic tract voxels (upper diagram) and the mean probabilistic connectivity distribution values of the synaesthete E.S. and the 10 professional musicians with absolute pitch for both hemispheres (lower diagram). Probabilities were derived from *z*-score transformations.

$p=0.115$ for the left and right hemisphere, respectively (Fig. 6, upper diagram). The mean connectivity distribution across all suprathreshold voxels was almost equal between the synaesthete and the musicians in the left hemisphere ($z=0.34$, $p=0.367$), but almost twice as much in the right hemisphere of E.S. compared with the average tractograph of the professional musicians with absolute pitch ($z=1.93$, $p=0.027$), a difference that is statistically significant (Fig. 6, lower diagram).

Discussion

As hypothesised, the comparison of the brain of the synaesthete E.S. with the brains of 17 professional musicians and with the brains of 20 normal control subjects revealed large structural differences in areas involved in the processing of both the inducing stimulus (auditory cortices) and the concurrent perceptions (gustatory and visual areas). Our results derived from two different imaging modalities (diffusion- and T1-weighted) and from two different comparison populations (normal control subjects and professional musicians with absolute pitch) converge in that they show a consistent pattern of bilateral brain differences in auditory areas (planum temporale and Heschl's gyrus), insular cortex, and occipital regions. In these particular brain regions, the multiple synaesthete E.S. shows increased FA accompanied by increased WM volumes and decreased GM volumes in the same regions. Complementary, probabilistic fibre tractography revealed hyperconnectivity in bilateral perisylvian-insular regions in the synaesthete E.S. compared with the average tractographs derived from the 10 female professional musicians with absolute pitch.

Our results provide strong evidence for a neuroanatomical basis to synaesthetic experiences in the interval-taste and the tone-colour synaesthesia, hence corroborating the proposed theory of increased anatomical connections between relevant brain areas as originally formulated for the grapheme-colour synaesthesia (Ramachandran and Hubbard, 2001; Hubbard et al., 2005). Our results further show that in addition to alterations in the connections between the relevant areas in the brain of the synaesthete E.S., there are structural anomalies within these areas. These anomalies may reinforce proposed neurophysiological mechanisms such as local crossactivation, disinhibition of feedback, or re-entrant of feedback. The neurophysiological mechanism that is evoked by this hyperconnectivity might be different between the interval-taste and tone-colour synaesthesia and cannot be investigated by structural neuroimaging.

The auditory cortices of the superior temporal gyri are the key structures for the processing of the inducing stimulus (music interval) (Hickok and Poeppel, 2007; Zatorre et al., 2007; Wu et al., 2008), and

the insulae (together with the parietal and frontal opercula) are the key structures for the processing of the concurrent perception (taste) (Nitschke et al., 2006; Small et al., 1999) in the interval-taste synaesthesia. In the tone-colour synaesthesia, the areas of the inducing stimulus (tone perception) are the same as in the interval-taste synaesthesia (auditory cortices), while the areas for the processing of the concurrent perception (colour) are the human colour processing areas (V4 and V4α) in the occipital lobes (Bartels and Zeki, 2000) and lower- and higher-order visual areas (Tootell et al., 2004) located in the ventral and dorsal visual processing stream. In the interval-taste synaesthesia, the areas for the processing of the inducing stimulus as well as the concurrent perception lay adjacent to each other, a fact that might facilitate the crossactivation mechanism. With respect to the tone-colour synaesthesia, the theory of local crossactivation cannot be applied because the two relevant brain areas are located further away from each other than the grapheme and colour centre for which the theory was originally proposed (Ramachandran and Hubbard, 2001; Hubbard and Ramachandran, 2005). This fact might make the local crossactivation mechanism less plausible in the tone-colour synaesthesia compared with the grapheme-colour and interval-taste synaesthesia. Therefore, another neurophysiological mechanism (e.g., re-entrant processing or disinhibition of feedback) for the tone-colour synaesthesia might be considered as being at work, although, instead of *local* crossactivation a *distal* (distant) crossactivation mechanism could be assumed.

Functional imaging studies in grapheme-colour synaesthesia, a frequent form of synaesthesia and therefore the most investigated synaesthesia type, revealed different patterns of activation in the colour processing area V4 and/or in the anterior (AIT) and posterior inferior temporal gyrus (PIT) in synaesthetes compared with non-synaesthetes (Paulesu et al., 1995; Nunn et al., 2002; Weiss et al., 2005; Rich et al., 2006). For example, when hearing words, word-colour synaesthetes showed activation in the colour centre V4/V8, whereas control subjects exhibited no such activation when imagining colours in response to spoken words (Nunn et al., 2002).

Hubbard et al. used functional magnetic resonance imaging (fMRI) to test the crossactivation hypothesis (Hubbard and Ramachandran, 2005) and found that in grapheme-colour synaesthetes both the visual word form area (VWFA) (Cohen and Dehaene, 2004) and the V4 complex were activated when viewing graphemes compared with viewing non-linguistic symbols (Hubbard et al., 2005). Other researchers have found similar results using fMRI and retinotopic as well as colour mapping (Sperling et al., 2006). Besides occipital areas, there is support for the involvement of parietal areas in grapheme-colour synaesthesia as revealed by electroencephalography (Beeli et al., 2007) and transcranial magnetic stimulation (Esterman et al., 2006).

To date, only one study has investigated the neural basis of synaesthesia with structural MRI (Rouw and Scholte, 2007). These authors used diffusion tensor imaging (DTI) to investigate fibre connectivity in 18 grapheme-colour synaesthetes and found increased structural connectivity in the right inferior temporal cortex, left superior parietal cortex, and bilateral superior frontal cortex in synaesthetes compared with non-synaesthetes. They concluded that this structural hyperconnectivity is associated with the presence of grapheme-colour synaesthesia, although they found no structural differences neither in the vicinity of the colour processing area nor in the VWFA in grapheme-colour synaesthetes compared with non-synaesthetes (Rouw and Scholte, 2007).

In interval-taste synaesthesia the increase in FA and the course of the tractographs in the right and left white matter areas that connects auditory areas with the insulae (lay immediately beneath these two areas) supports the theory of local crossactivation (Hubbard and Ramachandran, 2005) between these regions due to their increased neural connectivity. The increased WM volumes of E.S.'s brain in the right Heschl's gyrus/planum temporale complement the findings of the FA analysis and the tractography in these areas. In addition, the decreased GM volumes of the synaesthete in the left insula and left superior temporal gyrus might facilitate the local crossactivation mechanism (Ramachandran and Hubbard, 2001; Hubbard and Ramachandran, 2005). Reduced GM volumes in auditory areas in a person with absolute pitch perception are an unexpected finding (Luders et al., 2004). However, the interval-taste synaesthesia of E.S. might have caused a cortical reorganisation of a kind different from the reorganisation shown in auditory areas by musicians with absolute pitch (Luders et al., 2004). E.S. uses her interval-taste and tone-colour synaesthesia to identify musical intervals and the pitch of a tone, this possibly being a cognitive problem-solving mechanism, applied specifically by E.S. when forced to identify tones or musical intervals and rendering a reorganisation of her auditory areas unnecessary.

Besides the GM and WM volume differences found in the synaesthete's brain in the auditory areas, we found increased FA in the right superior occipital gyrus of E.S. (Fig. 1c) compared with normal control subjects and in both lateral occipital cortices compared with professional musicians (Fig. 1f). Additionally, increased WM and GM volumes in different posterior occipital and temporo-occipital areas (see Tables 1 and 2) support an anatomical basis even for the tone-colour synaesthesia. Although there were no significant differences in the vicinity of the colour processing areas, it is obvious that there are large structural differences (in FA as well as in GM and WM volumes) in many lower- and higher-order visual areas located in both the ventral and dorsal visual processing stream, that help to explain the occurrence of the concurrent colour perception in E.S (re-entrant processing). Especially, comparing E.S. with the professional musicians showed a cluster with increased WM volume in the right intracalcarine cortex (V1), the left optic radiation in the cuneal region, and the right optic radiation near the hippocampus (Table 2). Furthermore, the same comparison revealed increased GM volume in the left (Fig. 3f) and right lateral occipital cortex and in both occipital poles (V2). Our results may suggest the involvement of subcortical structures in synaesthesia by showing increased GM volumes in both thalami of E.S. These increased thalamic GM volumes might be rather related to the kind of instrument they play (flute player versus keyboard and string players) than to her synaesthetic experiences, because these thalamic differences were predominately found in the comparison with the professional musicians. With the exception of one small WM volume cluster found in the right middle temporo-occipital gyrus and one small FA cluster found in the right lateral occipital gyrus, there were no significant clusters in the occipital lobes where normal control subjects or professional musicians showed increased GM or WM volumes or enhanced FA compared with the multiple synaesthete E.S. These structural differences found in the various occipital regions together with the alterations found in auditory areas (already reported above) represent the neuroarchitectonic basis for the tone-colour synaesthesia in the multiple synaesthete E.S.

Besides her different synaesthetic experiences, E.S. has also absolute pitch perception and is a professional musician (flute player). Several reports have revealed structural brain differences between musicians and non-musicians (Bengtsson et al., 2005; Keenan et al., 2001; Gaser and Schlaug, 2003; Schlaug et al., 1995; Hutchinson et al., 2003), particularly in auditory and sensorimotor areas. The comparison of E.S. with normal control subjects revealed anatomical differences in auditory areas that might also be explained by the fact that in addition to her two different forms of synaesthesia, E.S. is also a professional musician with absolute pitch perception. To unequivocally attribute the structural brain differences in the auditory areas of E.S. to her synaesthetic experiences we also compared her brain with brains of 17 professional female musicians (including 10 musicians with absolute pitch perception) to rule out any influence from musical training and absolute pitch on her auditory cortices. As

expected, we were able to replicate our findings derived from the comparisons with the normal control subjects. E.S. compared with professional musicians showed increased FA in the left planum temporale and in both Heschl's gyri, decreased GM volume in both Heschl's gyri, right planum temporale, and right posterior superior temporal gyrus, and increased WM volumes in the left and right planum temporale, although there are also two small cluster (comprised by less than 100 mm^3 each) with decreased WM volumes in the right planum temporale and in the left superior temporal gyrus in the synaesthete (Table 2). However, it is quite clear that the auditory regions in the brain of E.S. differ significantly from the auditory areas typically found in professional musicians, although E.S. herself is a professional flute player.

The consistent finding of reduced GM and WM volumes and reduced FA of E.S. in areas of the pre- and postcentral gyri as revealed by both group comparisons is in stark contrast to findings from studies investigating the musician's brain (Gaser and Schlaug, 2003), specifically motor and sensorimotor areas in keyboard and string players (Amunts et al., 1997). This inconsistency might best be explained by the fact that E.S. is a professional flute player and not a keyboard or string player whose hand manipulations require comparatively greater strength and flexibility compared with the hand manipulations of flute players, hence no reorganisation of primary motor and somatosensory areas might have occurred. Alternatively, these differences could also be explained by less athletic activities of the synaesthete E.S. compared with the 20 normal control females. But differences in these motor and somatosensory regions are heterogeneous across imaging modalities (diffusion- versus. T1-weighted) as well as comparison groups (normal control subjects versus professional musicians).

Whether these structural brain differences are genetically determined still remains an open question. There is evidence for a genetic component because synaesthesia runs in families and is more frequent in females than in males, this suggesting, despite inconsistent findings (Smilek et al., 2002, 2005), an X-chromosomal linked dominant trait (Baron-Cohen et al., 1993, 1996; Harrison and Baron-Cohen, 1997; Bailey and Johnson, 1997; Ward and Simner, 2005). Whether these structural brain differences are caused by a failure in neural pruning (Kennedy et al., 1997; Rodman and Moore, 1997; Hubbard and Ramachandran, 2005) or even by synaptic sprouting as proposed to be the neurophysiological mechanism in an acquired form of synaesthesia (Armel and Ramachandran, 1999) remains to be shown.

However, the cellular basis of these macroscopic structural alterations is still not fully understood and cannot be investigated by structural neuroimaging. Such events may include synaptogenesis, dendritic expansion, myelin thickening, increased neuronal sizes, or the genesis of glial or even neuronal cells. We prefer to relate our finding of macroscopic brain differences to changes in myelo- and cytoarchitectonics because the T1-weighted MR intensity profiles have been shown to be best explained by a weighted sum of myeloarchotectonic and cytoarchitectonic profiles (Eickhoff et al., 2005). Imaging results have to be compared with histological data for identification of the structural basis at the microscopic level.

Our results also highlight the power of combining complementary MR imaging methods that based on different magnetic resonance sensitive properties of the tissue under investigation, that is, methods measuring the diffusion characteristics of protons in the WM on one hand (investigated with DTI) and methods measuring the volumetric properties of WM and GM on the other hand (investigated with T1-weighted MRI). Converging results were obtained as shown in Fig. 4.

We also included seven professional female musicians without absolute pitch in the musician control group in order to increase the number of professional musicians and hence render the musician group more representative which is very important when deriving *z*-scores that are dependent on the mean and standard deviation image of the group. Furthermore, the synaesthete E.S. reported that she identifies pure tones as well as musical intervals by her two types of synaesthesia, hence we did not expected any neural reorganisation in the brain of E.S. that is related to her absolute pitch perception.

There was a large (1900 voxels in size) and highly significant (mean *z*-score = −4.05; minimum *z*-score = −6.27) cluster with decreased FA in the genu of the corpus callosum in the brain of the synaesthete E.S. compared with the normal control females (but not when compared with the professional musicians). However, we will not discuss this cluster further for the following four reasons: (i) structural differences in the corpus callosum were not a priori hypothesised. (ii) The standard deviation of the *z*-scores in this cluster was very large (S.D. = 0.759). (iii) Decreased FA in the genu of the corpus callosum when comparing a musician with non-musicians contradicts the literature (Schmithorst and Wilke, 2002). (iv) Because it was only found in comparison with normal controls, but not when E.S. was compared with professional musicians, suggesting that this difference is related to her musical abilities and not to her types of synaesthesia.

A potential limitation of our study is rooted in the fact that the interval-taste synaesthesia, which is a very rare type of synaesthesia, was investigated only in a single subject, hence limiting the generalization of our findings. A further potential limitation is that we report probabilities ($p<0.001$) that were not corrected for the multiple comparisons problem that we encountered. But our more liberal threshold can be justified by the following four reasons: (i) there were strong a priori hypotheses about the locations where we expected structural brain differences; (ii) we faced *z*-scores for many of the structural differences in the range of 4 to 5 (−4 to −5) corresponding to a range of probabilities between $p=0.00003$ (1 out of 31,574) and $p=0.0000003$ (1 out of 3,486,914). Such large *z*-scores represent strong effect sizes and such small probabilities can be considered as corrected for multiple comparisons, i.e., the local statistical maxima that we reported would survive a multiple comparison correction procedure such as family-wise error correction. (iii) The fact that we replicated our results found in one sample (normal control subjects) with another sample (professional musicians) mitigates the need of correcting the error probability for multiple comparisons. (iv) We are not aware of any implementation of such a correction algorithm that computes the number of resels (resolution elements) when comparing a single subject with a group outside the classical neuroimaging software packages such as SPM and FSL that contain these correction procedures.

We revealed first findings to indicate the neuroanatomical basis of both the interval-taste and tone-colour synaesthesia, at least in the multiple synaesthete E.S., thus extending current knowledge about the neural underpinnings of the different forms of synaesthesia. Our results are partially in line with those of the first structural neuroimaging study that focussed on a more common form of synaesthesia, grapheme-colour synaesthesia (Rouw and Scholte, 2007). Our findings might have implications for the understanding of human perception in general and of multimodal integration specifically, and may encourage similar research into dysfunctional perceptual phenomenon such as hallucinations in schizophrenics or in Charles Bonnet syndrome (e.g., Whitford et al. 2007).

Acknowledgments

This work was supported in part by a grant from the NCCR (National Centre of Competence in Research) Neural Plasticity and Repair (grant to L.J.), Swiss National Science Foundation (SNF). We thank our synaesthete E.S. for her collaboration, the control subjects, and the professional musicians for their participation in the study, and the master students Benedikt Brönimann and Rafael Huber for their assistance in data analysis and visualisation. We also thank Marcus Cheetham for improving the English manuscript and the two anonymous reviewers for their helpful comments.

Appendix A. Supplementary data

Supplementary data associated with this article can be found, in the online version, at doi:10.1016/j.neuroimage.2008.07.018.

References

Amunts, K., Schlaug, G., Jancke, L., Steinmetz, H., Schleicher, A., Dabringhaus, A., Zilles, K., 1997. Motor cortex and hand motor skills: structural compliance in the human brain. Hum. Brain Mapp. 5, 206–215.

Armel, K.C., Ramachandran, V.S., 1999. Acquired synaesthesia in retinitis pigmentosa. Neurocase 293–296.

Ashburner, J., Friston, K.J., 2000. Voxel-based morphometry—the methods. Neuroimage 11, 805–821.

Ashburner, J., Friston, K.J., 2005. Unified segmentation. Neuroimage 26, 839–851.

Bailey, M.E.S., Johnson, K.J., 1997. Synaesthesia: is a genetic analysis feasible. In: Baron-Cohen, S., Harrison, J.E. (Eds.), Synaesthesia: Classic and Contemporary Readings. Blackwell, Oxford, England, pp. 182–207.

Baron-Cohen, S., Harrison, J., Goldstein, L.H., Wyke, M., 1993. Coloured speech perception: Is synaesthesia what happens when modularity breaks down. Perception 22, 419–426.

Baron-Cohen, S., Burt, L., Smith-Laittan, F., Harrison, J., Bolton, P., 1996. Synaesthesia: prevalence and familiality. Perception 25, 1073–1079.

Bartels, A., Zeki, S., 2000. The architecture of the colour centre in the human visual brain: new results and a review. Eur. J. Neurosci. 12, 172–193.

Beeli, G., Esslen, M., Jäncke, L., 2005. Synaesthesia: when coloured sounds taste sweet. Nature 434, 38.

Beeli, G., Esslen, M., Jäncke, L., 2007. Time course of neural activity correlated with colored-hearing synesthesia. Cereb. Cortex 18 (2), 379–385.

Behrens, T.E.J., Johansen-Berg, H., Jbabdi, S., Rushworth, M.F.S., Woolrich, M.W., 2007. Probabilistic diffusion tractography with multiple fibre orientations: what can we gain. Neuroimage 34, 144–155.

Behrens, T.E.J., Woolrich, M.W., Jenkinson, M., Johansen-Berg, H., Nunes, R.G., Clare, S., Matthews, P.M., Brady, J.M., Smith, S.M., 2003a. Characterization and propagation of uncertainty in diffusion-weighted MR imaging. Magn. Reson. Med. 50, 1077–1088.

Behrens, T.E.J., Johansen-Berg, H., Woolrich, M.W., Smith, S.M., Wheeler-Kingshott, C.A.M., Boulby, P.A., Barker, G.J., Sillery, E.L., Sheehan, K., Ciccarelli, O., Thompson, A.J., Brady, J.M., Matthews, P.M., 2003b. Non-invasive mapping of connections between human thalamus and cortex using diffusion imaging. Nat. Neurosci. 6, 750–755.

Bengtsson, S.L., Nagy, Z., Skare, S., Forsman, L., Forssberg, H., Ullén, F., 2005. Extensive piano practicing has regionally specific effects on white matter development. Nat. Neurosci. 8, 1148–1150.

Cohen, L., Dehaene, S., 2004. Specialization within the ventral stream: the case for the visual word form area. Neuroimage 22, 466–476.

Cuadra, M.B., Cammoun, L., Butz, T., Cuisenaire, O., Thiran, J.-P., 2005. Comparison and validation of tissue modelization and statistical classification methods in T1-weighted MR brain images. IEEE Trans. Med. Imaging 24, 1548–1565.

Eickhoff, S., Walters, N.B., Schleicher, A., Kril, J., Egan, G.F., Zilles, K., Watson, J.D.G., Amunts, K., 2005. High-resolution MRI reflects myeloarchitecture and cytoarchitecture of human cerebral cortex. Hum. Brain Mapp. 24, 206–215.

Esterman, M., Verstynen, T., Ivry, R.B., Robertson, L.C., 2006. Coming unbound: disrupting automatic integration of synesthetic color and graphemes by transcranial magnetic stimulation of the right parietal lobe. J. Cogn. Neurosci. 18, 1570–1576.

Gaab, N., Schulze, K., Ozdemir, E., Schlaug, G., 2006. Neural correlates of absolute pitch differ between blind and sighted musicians. Neuroreport 17, 1853–1857.

Gaser, C., Schlaug, G., 2003. Brain structures differ between musicians and non-musicians. J. Neurosci. 23 (27), 9240–9245.

Grossenbacher, P.G., Lovelace, C.T., 2001. Mechanisms of synesthesia: cognitive and physiological constraints. Trends Cogn. Sci. 5, 36–41.

Hadjikhani, N., Liu, A.K., Dale, A.M., Cavanagh, P., Tootell, R.B.H., 1998. Retinotopy and color sensitivity in human visual cortical area V8. Nat. Neurosci. 1, 235–241.

Hamilton, R.H., Pascual-Leone, A., Schlaug, G., 2004. Absolute pitch in blind musicians. Neuroreport 15, 803–806.

Harrison, J.E., Baron-Cohen, S., 1997. Synaesthesia: A review of psychological theories. In: Baron-Cohen, S., Harrison, J.E. (Eds.), Synaesthesia: Classic and Contemporary Readings. Blackwell, Oxford, England, pp. 109–122.

Hickok, G., Poeppel, D., 2007. The cortical organization of speech processing. Nat. Rev. Neurosci. 8, 393–402.

Hubbard, E.M., Ramachandran, V.S., 2005. Neurocognitive mechanisms of synesthesia. Neuron 48, 509–520.

Hubbard, E.M., Arman, A.C., Ramachandran, V.S., Boynton, G.M., 2005. Individual differences among grapheme-color synesthetes: brain-behavior correlations. Neuron 45, 975–985.

Hutchinson, S., Hui-Lin Lee, L., Gaab, N., Schlaug, G., 2003. Cerebellar volume of musicians. Cereb. Cortex 13, 943–947.

Keenan, J.P., Thangaraj, V., Halpern, A.R., Schlaug, G., 2001. Absolute pitch and planum temporale. Neuroimage, 14 (6), 1402–1408.

Kennedy, H., Batardiere, A., Dehay, C., Barone, P., 1997. Synaesthesia: implications for developmental neurobiology. In: Baron-Cohen, S., Harrison, J.E. (Eds.), Synaesthesia: Classic and Contemporary Readings. Blackwell, Oxford, England, pp. 243–256.

Luders, E., Gaser, C., Jäncke, L., Schlaug, G., 2004. A voxel-based approach to gray matter asymmetries. Neuroimage 22, 656–664.

Nitschke, J.B., Dixon, G.E., Sarinopoulos, I., Short, S.J., Cohen, J.D., Smith, E.E., Kosslyn, S.M., Rose, R.M., Davidson, R.J., 2006. Altering expectancy dampens neural response to aversive taste in primary taste cortex. Nat. Neurosci. 9, 435–442.

Nunn, J.A., Gregory, L.J., Brammer, M., Williams, S.C.R., Parslow, D.M., Morgan, M.J., Morris, R.G., Bullmore, E.T., Baron-Cohenm, S., Gray, J.A., 2002. Functional magnetic resonance imaging of synesthesia: activation of V4/V8 by spoken words. Nat. Neurosci. 5, 371–375.

Paulesu, E., Harrison, J., Baron-Cohen, S., Watson, J.D.G., Goldstein, L., 1995. The physiology of coloured hearing. A PET activation study of colour-word synaesthesia. Brain 118, 1073.

Pierce, A.H., 1907. Gustatory audition: a hitherto undescribed variety of synaesthesia. Am. J. Psychol. 18, 341–352.

Ramachandran, V.S., Hubbard, E.M., 2001. Psychophysical investigations into the neural basis of synaesthesia. Proc. Biol. Sci. 268, 979–983.

Rich, A.N., Mattingley, J.B., 2002. Anomalous perception in synaesthesia: a cognitive neuroscience perspective. Nat. Rev. Neurosci. 3, 43–52.

Rich, A.N., Williams, M.A., Puce, A., Syngeniotis, A., Howard, M.A., McGlone, F., Mattingley, J.B., 2006. Neural correlates of imagined and synaesthetic colours. Neuropsychologia 44, 2918–2925.

Rodman, H., Moore, T., 1997. Development and plasticity of extrastriate visual cortex in monkeys. In: Rockland, K.S., Kaas, J.H., Peters, A. (Eds.), Cerebral Cortex. Plenum Press, New York, pp. 639–672.

Rouw, R., Scholte, H.S., 2007. Increased structural connectivity in grapheme-color synesthesia. Nat. Neurosci. 10, 792–797.

Schlaug, G., Jäncke, L., Huang, Y., Steinmetz, H., 1995. In Vivo Evidence of Structural Brain Asymmetry in Musicians. Science 267, 699–701.

Schmithorst, V.J., Wilke, M., 2002. Differences in white matter architecture between musicians and non-musicians: a diffusion tensor imaging study. Neurosci. Lett. 321, 57–60.

Simner, J., 2007. Beyond perception: synaesthesia as a psycholinguistic phenomenon. Trends Cogn. Sci. 11, 23–29.

Simner, J., Ward, J., 2006. Synaesthesia: the taste of words on the tip of the tongue. Nature 444, 438.

Small, D.M., Zald, D.H., Jones-Gotman, M., Zatorre, R.J., Pardo, J.V., Frey, S., Petrides, M., 1999. Human cortical gustatory areas: a review of functional neuroimaging data. Neuroreport 10, 7–14.

Smilek, D., Dixon, M.J., Cudahy, C., Merikle, P.M., 2001. Synaesthetic photisms influence visual perception. J. Cogn. Neurosci. 13, 930–936.

Smilek, D., Moffatt, A., Pasternak, J., White, B.N., Dixon, M.J., Merikle, P.M., 2002. Synaesthesia: A case study of discordant monozygotic twins. Neurocase 8, 338–342.

Smilek, D., Dixon, M.J., Merikle, P.M., 2005. Synaesthesia: discordant male monozygotic twins. Neurocase 11, 363–370.

Smith, S.M., Jenkinson, M., Woolrich, M.W., Beckmann, C.F., Behrerns, T.E.J., Johansen-Berg, H., Bannister, P.R., de Luca, M., Drobnjak, I., Flitney, D.E., Niazy, R.K., Saunders, J., Vickers, J., Zhang, Y., de Stefano, N., Brady, J.M., Matthews, P.M., 2004. Advances in functional and structural MR image analysis and implementation as FSL. Neuroimage 23, S208–S219.

Smith, S.M., Jenkinson, M., Johanes-Berg, H., Rueckert, D., Nichols, T.E., Mackay, C.E., Watkins, K.E., Ciccarelli, O., Cader, M.C., Matthews, P.M., Behrens, T.E.J., 2006. Tract-based spatial statistics: voxelwise analysis of multi-subject diffusion data. Neuroimage 31, 1487–1505.

Sperling, J.M., Prvulovic, D., Linden, D.E.J., Singer, W., Stirn, A., 2006. Neuronal correlates of colour-graphemic synaesthesia: A fMRI study. Cortex 42, 295–303.

Tootell, R.B.H., Nelissen, K., Vanduffel, W., Orban, G.A., 2004. Search for color 'center(s)' in macaque visual cortex. Cereb. Cortex 14, 353–363.

Ward, J., Simner, J., 2003. Lexical-gustatory synaesthesia: linguistic and conceptual factors. Cognition 89, 237–261.

Ward, J., Simner, J., 2005. Is synaesthesia an X-linked dominant trait with lethality in males. Perception 34, 611–623.

Weiss, P.H., Zilles, K., Fink, G.R., 2005. When visual perception causes feeling: enhanced cross-modal processing in grapheme-color synesthesia. Neuroimage 28, 859–868.

Whitford, T.J., Farrow, T.F.D., Rennie, C.J., Grieve, S.M., Gomes, L., Brennan, J., Harris, A.W.F., Williams, L.M., 2007. Longitudinal changes in neuroanatomy and neural activity in early schizophrenia. Neuroreport 18, 435–439.

Wu, C., Kirk, I.J., Hamm, J.P., Lim, V.K., 2008. The neural networks involved in pitch labeling of absolute pitch musicians. Neuroreport 19, 851–854.

Zatorre, R.J., Chen, J.L., Penhune, V.B., 2007. When the brain plays music: auditory-motor interactions in music perception and production. Nat. Rev. Neurosci. 8, 547–558.